Supporting Information

Highly efficient As(V)/Sb(V) removal by magnetic sludge composite: synthesis, characterization, equilibrium, and mechanism studies

Li Wang , Jing-Mei Wang , Ren Zhang , Xin-Gang Liu , Guo-Xin Song , Xiao-Feng Chen , Yi Wang*, Ji-Lie Kong

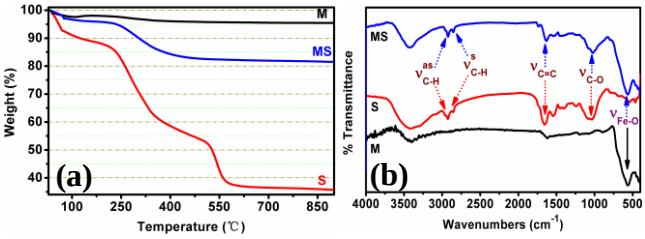

Fig. S1 (a) TG curves and (b) FTIR spectra of sludge (S), pristine magnetite nanoparticles (M), and magnetic sludge (MS).

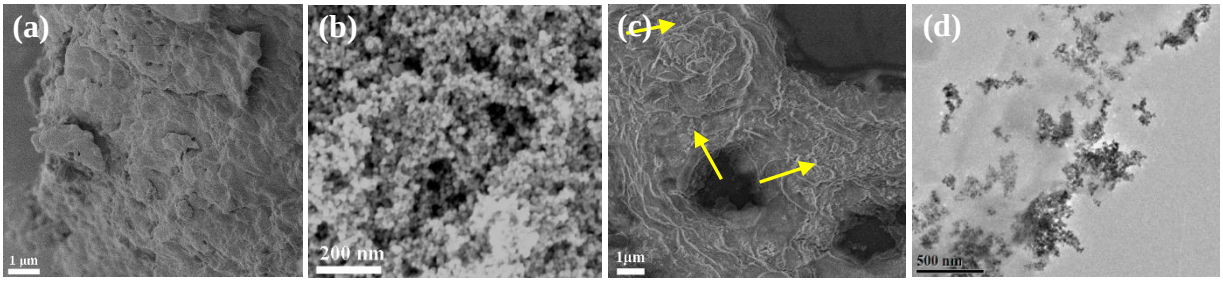

Fig. S2 (a–c) SEM images of (a) Lyophilized activated sludge (S), (b) Pristine magnetite nanoparticles (M), and (c) Magnetic sludge (MS). (d) TEM images of magnetic sludge (MS).

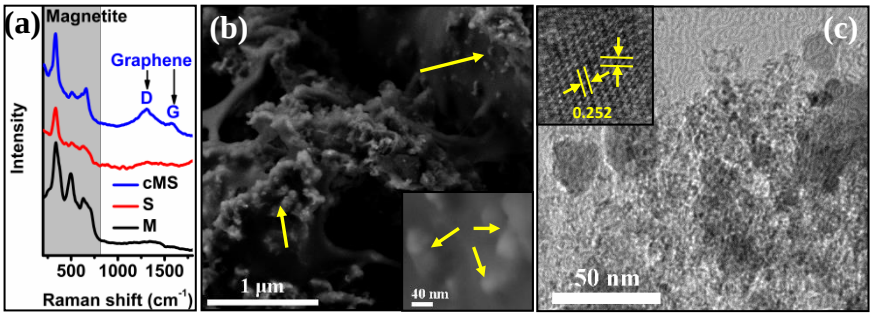

Fig. S3 (a) Raman spectrum of sludge (S), pristine magnetite NPs (M), and calcined magnetic sludge(cMS). (b)

SEM image of cMS, with the inset and arrows highlighting the Fe_3O_4 nanoparticles. (c) TEM image of cMS with an inset showing a HRTEM image of the confined nanoparticles.

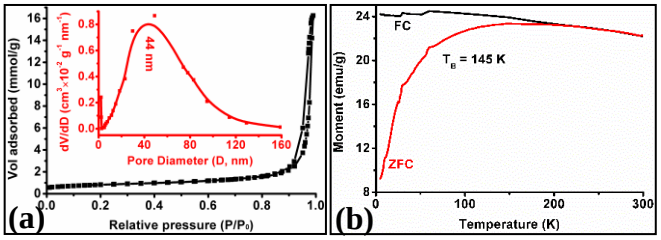

Fig. S4 (a) N_2 adsorption–desorption isotherm and pore size distribution curve (inset) for the magnetic sludge. (b) Zero-field-cooled and field-cooled magnetization curves of the magnetic sludge under an applied magnetic field intensity (H) of 300 Oe.

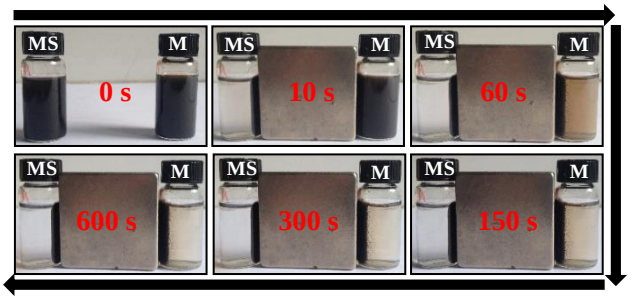

Fig. S5 Images of pristine magnetite nanoparticles (M) and magnetic sludge (MS) in the presence of a magnet for different time periods.

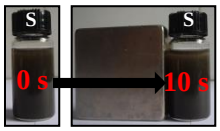

Fig. S6 Images of sludge in the absence (left) and presence (right) of a magnet.

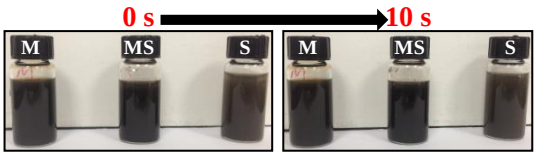

Fig. S7 Images of sludge (S), pristine magnetite nanoparticles (M), and magnetic sludge (MS) in the absence of a magnet.

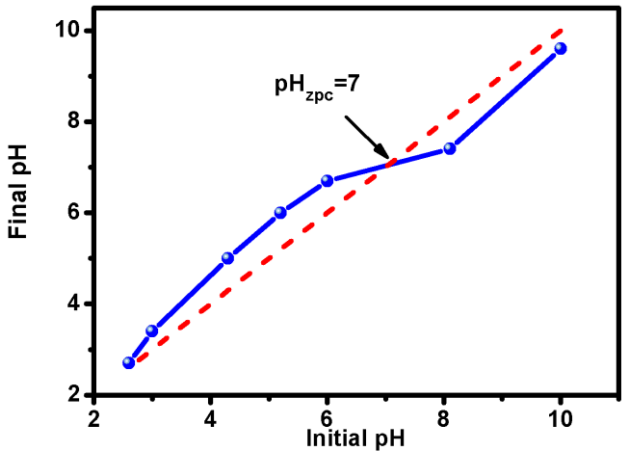

Fig. S8 Zero point of charge for the magnetic sludge.